



## LJMU Research Online

Che, HS, Levi, E, Jones, M, Hew, W-P and Abd Rahim, N

**Current Control Methods for an Asymmetrical Six-Phase Induction Motor Drive**

<http://researchonline.ljmu.ac.uk/id/eprint/114/>

### Article

**Citation** (please note it is advisable to refer to the publisher's version if you intend to cite from this work)

**Che, HS, Levi, E, Jones, M, Hew, W-P and Abd Rahim, N (2014) Current Control Methods for an Asymmetrical Six-Phase Induction Motor Drive. IEEE TRANSACTIONS ON POWER ELECTRONICS, 29 (1). pp. 407-417. ISSN 0885-8993**

LJMU has developed [LJMU Research Online](#) for users to access the research output of the University more effectively. Copyright © and Moral Rights for the papers on this site are retained by the individual authors and/or other copyright owners. Users may download and/or print one copy of any article(s) in LJMU Research Online to facilitate their private study or for non-commercial research. You may not engage in further distribution of the material or use it for any profit-making activities or any commercial gain.

The version presented here may differ from the published version or from the version of the record. Please see the repository URL above for details on accessing the published version and note that access may require a subscription.

For more information please contact [researchonline@ljmu.ac.uk](mailto:researchonline@ljmu.ac.uk)

<http://researchonline.ljmu.ac.uk/>

# Current Control Methods for an Asymmetrical Six-phase Induction Motor Drive

Hang Seng Che, Emil Levi, *Fellow, IEEE*, Martin Jones, Wooi Ping Hew,  
Nasrudin Abd. Rahim, *Senior Member, IEEE*

**Abstract**—Using the vector space decomposition (VSD) approach, the currents in a multiphase machine with distributed winding can be decoupled into the flux and torque producing  $\alpha$ - $\beta$  components, and the loss-producing  $x$ - $y$  and zero-sequence components. While the control of  $\alpha$ - $\beta$  currents is crucial for flux and torque regulation, control of  $x$ - $y$  currents is important for machine/converter asymmetry and dead-time effect compensation. In this paper, an attempt is made to provide a physically meaningful insight into current control of a six-phase machine, by showing that the fictitious  $x$ - $y$  currents can be physically interpreted as the circulating currents between the two three-phase windings. Using this interpretation, the characteristics of  $x$ - $y$  currents due to the machine/converter asymmetry can be analysed. The use of different types of  $x$ - $y$  current controllers for asymmetry compensation and suppression of dead time induced harmonics is then discussed. Experimental results are provided throughout the paper, to underpin the theoretical considerations, using tests on a prototype asymmetrical six-phase induction machine.

**Index Terms**— Induction motor drives, Multiphase systems, Current control

## I. INTRODUCTION

USING the vector space decomposition (VSD) approach, an  $n$ -phase machine can be represented using  $n/2$  (or  $(n-1)/2$  for machines with an odd number of phases) orthogonal subspaces, which include one  $\alpha$ - $\beta$  subspace and several  $x$ - $y$  subspaces, and the zero-sequence components [1]. For a machine with sinusoidal magneto-motive force distribution, only the  $\alpha$ - $\beta$  components contribute to useful electro-mechanical energy conversion, while  $x$ - $y$  and zero-sequence components only produce losses. In most cases, zero-sequence components can be neglected, since the neutral point of the machine is usually isolated so that the zero-sequence

currents cannot flow. Due to the existence of additional degrees of freedom, controlling only the torque and flux producing  $\alpha$ - $\beta$  currents is insufficient and additional controllers are necessary to nullify the  $x$ - $y$  currents that may flow due to the machine/converter asymmetry and the inverter dead-time effect [2].

Among the multiphase machines, those with multiple three-phase windings (such as six-phase, nine-phase or eighteen-phase machine), are most frequently discussed. While having the benefits of a multiphase machine, the modular three-phase structures allow the use of the well established three-phase technology. This study hence focuses on the discussion of  $x$ - $y$  current control for an asymmetrical six-phase machine ( $30^\circ$  spatial shift between the two three-phase stator windings) with isolated neutral points.

Unlike in multiphase machines with a prime number of phases, where  $x$ - $y$  currents are fictitious, the  $x$ - $y$  currents in a six-phase machine can have more meaningful physical interpretation. As will be shown in Section II, the  $x$ - $y$  currents can be interpreted as the circulating currents between the two three-phase windings in a six-phase machine. Using this concept, the control of  $x$ - $y$  currents can be analysed.

The paper is organised as follows. Section II establishes the physical interpretation of the  $x$ - $y$  currents, based on the VSD and double- $dq$  machine models. Section III discusses the two roles of the  $x$ - $y$  current controllers: asymmetry compensation and dead-time effect compensation. Next, experimental results are given in Section IV, where the performance of several different types of  $x$ - $y$  current controllers is compared, in order to validate the analysis of Section III. Finally, conclusions of the work are summarised in Section V.

## II. INTERPRETATION OF THE X-Y CURRENTS USING VSD AND DOUBLE-DQ MODELLING APPROACHES

In the early studies of the asymmetrical six-phase machines, double- $dq$  or double-stator modelling approach has been utilised to aid the understanding of the machine's operation [3], [4]. Using this model, the two three-phase windings in a six-phase machine are treated separately. Two three-phase decoupling (Clarke) transformations are applied separately on the phase variables for each three-phase winding. This transforms the six-phase variables into two sets of stationary reference frame variables, denoted as  $\alpha_1$ - $\beta_1$  and  $\alpha_2$ - $\beta_2$  components, for windings 1 and 2, respectively:

$$\begin{bmatrix} f_{\alpha_1} & f_{\beta_1} \end{bmatrix}^T = [T_{\alpha\beta 1}] \begin{bmatrix} f_{a_1} & f_{b_1} & f_{c_1} \end{bmatrix}^T \quad (1)$$

$$\begin{bmatrix} f_{\alpha_2} & f_{\beta_2} \end{bmatrix}^T = [T_{\alpha\beta 2}] \begin{bmatrix} f_{a_2} & f_{b_2} & f_{c_2} \end{bmatrix}^T \quad (2)$$

Symbol  $f$  represents arbitrary machine variables (voltage,

Manuscript received September 11, 2012; revised January 10, 2013. Accepted February 6, 2013.

H.S. Che is with the University of Malaya, UMPEDAC Research Centre, Kuala Lumpur, Malaysia and with Liverpool John Moores University, School of Engineering, Technology and Maritime Operations, Liverpool L3 3AF, U.K. (e-mail: [cehase@hotmail.com](mailto:cehase@hotmail.com)).

E. Levi and M. Jones are with the School of Engineering, Technology and Maritime Operations, Liverpool John Moores University, Liverpool L3 3AF, U.K. (e-mails: [e.levi@ljmu.ac.uk](mailto:e.levi@ljmu.ac.uk) and [m.jones2@ljmu.ac.uk](mailto:m.jones2@ljmu.ac.uk)).

N.A. Rahim and W.P. Hew are with the UMPEDAC Research Centre, Wisma R&D, University of Malaya, 59990 Kuala Lumpur, Malaysia (e-mails: [nasrudin@um.edu.my](mailto:nasrudin@um.edu.my) and [wpheuw@um.edu.my](mailto:wpheuw@um.edu.my)).

current or flux). The spatial 30° displacement between the two windings is accounted for in the decoupling transformation. For an asymmetrical six-phase machine, the power invariant transformation for windings 1 and 2, respectively, is given with:

$$[T_{\alpha\beta 1}] = \sqrt{\frac{2}{3}} \begin{bmatrix} 1 & -\frac{1}{2} & -\frac{1}{2} \\ 0 & \frac{\sqrt{3}}{2} & -\frac{\sqrt{3}}{2} \end{bmatrix} \quad (3)$$

$$[T_{\alpha\beta 2}] = \sqrt{\frac{2}{3}} \begin{bmatrix} \frac{\sqrt{3}}{2} & -\frac{\sqrt{3}}{2} & 0 \\ \frac{1}{2} & \frac{1}{2} & -1 \end{bmatrix} \quad (4)$$

Vector space decomposition (VSD) [5] provides an alternative approach for describing the operation of a six-phase machine. Using the VSD model, a six-phase machine can be represented using three orthogonal sub-spaces, i.e. the  $\alpha$ - $\beta$ ,  $x$ - $y$  and zero-sequence subspaces. This approach gives an alternative description of the machine, which is useful for machine control and for development of pulse width modulation techniques. Harmonics of different orders are mapped into different subspaces. Furthermore, unlike the double- $dq$  model, the VSD model is applicable to multiphase machines with any phase number. It was noted in [6] that vector control using double- $dq$  and VSD approach gives very similar performance. However, the former requires voltage decoupling terms that are more complicated. Due to the advantages of the VSD model, including clear information on the harmonic mapping, most of the recent works related to multiphase machines (including this paper) are based on this approach. The relationship between VSD variables and phase variables for an asymmetrical six-phase machine with isolated neutrals is given with (zero-sequence components are omitted due to the isolated neutral points)

$$[f_\alpha \ f_\beta \ f_x \ f_y]^T = [T_{\alpha\beta}] [f_{a1} \ f_{b1} \ f_{c1} \ f_{a2} \ f_{b2} \ f_{c2}]^T \quad (5)$$

where  $[T_{\alpha\beta}]$  is the decoupling transformation

$$[T_{\alpha\beta}] = \frac{1}{\sqrt{3}} \begin{bmatrix} 1 & -\frac{1}{2} & -\frac{1}{2} & \frac{\sqrt{3}}{2} & -\frac{\sqrt{3}}{2} & 0 \\ 0 & \frac{\sqrt{3}}{2} & -\frac{\sqrt{3}}{2} & \frac{1}{2} & \frac{1}{2} & -1 \\ 1 & -\frac{1}{2} & -\frac{1}{2} & -\frac{\sqrt{3}}{2} & \frac{\sqrt{3}}{2} & 0 \\ 0 & -\frac{\sqrt{3}}{2} & \frac{\sqrt{3}}{2} & \frac{1}{2} & \frac{1}{2} & -1 \end{bmatrix} \quad (6)$$

Despite the various advantages of the VSD model, the variables are more difficult to interpret physically, unlike in the double- $dq$  model where  $\alpha$ 1- $\beta$ 1 variables are clearly related to the winding 1 and  $\alpha$ 2- $\beta$ 2 variables to the winding 2 of the machine. It is therefore desirable to provide a better physical interpretation of the VSD model variables by relating them with variables in the double- $dq$  model. This can be done by simply comparing the decoupling transformation matrices for the two methods.

By comparing equations (3) and (4) with (6), it can be seen that  $\alpha$ - $\beta$  components in the VSD model are proportional to the sum of the  $\alpha$ 1-,  $\alpha$ 2- and  $\beta$ 1-,  $\beta$ 2- components of the double- $dq$  model. On the other hand,  $x$ -component and  $y$ -component are proportional to the difference between  $\alpha$ 1-,  $\alpha$ 2- and  $\beta$ 1-,  $\beta$ 2- components, respectively, with the signs for the  $x$ - and  $y$ -

components inverted. As will be shown later, this opposite sign influences the rotational direction of the  $x$ - $y$  current phasor caused by the machine/converter asymmetry. The relationship is given with:

$$\begin{aligned} f_\alpha &= \sqrt{\frac{1}{2}}(f_{\alpha 1} + f_{\alpha 2}) = \sqrt{\frac{1}{2}}\Sigma f_\alpha \\ f_\beta &= \sqrt{\frac{1}{2}}(f_{\beta 1} + f_{\beta 2}) = \sqrt{\frac{1}{2}}\Sigma f_\beta \\ f_x &= \sqrt{\frac{1}{2}}(f_{\alpha 1} - f_{\alpha 2}) = \sqrt{\frac{1}{2}}\Delta f_\alpha \\ f_y &= \sqrt{\frac{1}{2}}(-f_{\beta 1} + f_{\beta 2}) = -\sqrt{\frac{1}{2}}\Delta f_\beta \end{aligned} \quad (7)$$

### III. X-Y CURRENT CONTROL FOR SIX-PHASE INDUCTION MACHINE

#### A. Asymmetry Compensation

The general structure of the current controllers within the rotor flux oriented control scheme, considered further on and based on VSD approach, is shown in Fig. 1. Here  $x$ - $y$  currents are not rotationally transformed and are shown as being controlled in the stationary reference frame.

As shown in [7], asymmetry in the machine windings or converter can cause large current distortion in the six-phase machine. Pulse width modulation (PWM) can also cause current distortion [8], but this effect is marginal if the proper PWM technique is chosen. With the effect from PWM minimised, the machine/converter asymmetry leads to the current flow in the  $x$ - $y$  plane, so proper  $x$ - $y$  current control has to be used to mitigate the problem. Several  $x$ - $y$  current control strategies have been proposed as a possible solution, including the use of resonant controllers [9] and PI controllers [10–12]. In particular, the PI controller is the favourable choice for  $x$ - $y$  currents control, due to its simple structure and well-known characteristics.

It has been shown in [10] that  $x$ - $y$  currents, produced by asymmetry in a five-phase machine, appear as ac components at synchronous frequency. By applying a rotational transformation which rotates the  $x$ - $y$  currents in the synchronous direction, the transformed  $x$ - $y$  currents will appear as a combination of dc and ac components. The use of PI controllers in this synchronous reference frame will compensate the dc component. However, due to the characteristics of the PI controllers, the ac component will

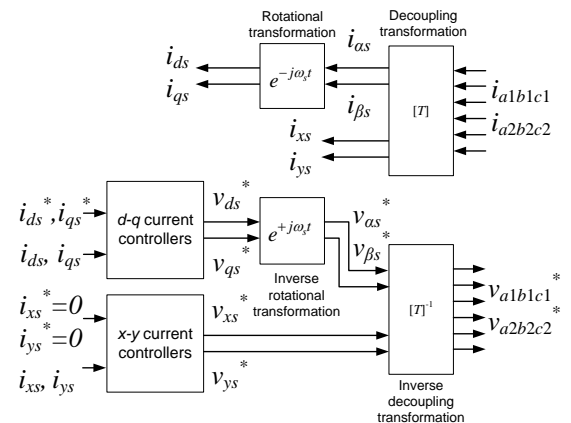


Fig. 1. General structure of the current controllers for a six-phase induction machine (rotational transformation is only applied to  $\alpha$ - $\beta$  components).

only be suppressed to an extent dictated by the controllers' bandwidth. In [11], it was shown that the effectiveness of asymmetry compensation using PI controllers depends on the type of asymmetry present. Here, this concept is reinforced using a more general analysis, showing that the  $x$ - $y$  currents due to the machine/converter asymmetry can be fully described using the concept of symmetrical components and the concept of  $x$ - $y$  currents discussed in Section II.

The six-phase currents of the six-phase machine are first separately considered as two sets of three-phase currents. If the double- $dq$  transformation (3)-(4) is applied to these currents,  $\alpha 1$ - $\beta 1$  and  $\alpha 2$ - $\beta 2$  currents are obtained. For ideal machine/converter without any asymmetry, the  $\alpha 1$ - $\beta 1$  and  $\alpha 2$ - $\beta 2$  currents form circular trajectories that are identical in radius and rotate at the same angular frequency  $+\omega_s$ . Both  $\alpha 1$ - $\beta 1$  and  $\alpha 2$ - $\beta 2$  currents can be represented by a positive sequence component,  $\vec{I}_{\alpha\beta+}$ , which is a rotating space phasor.

However, if there is an imbalance due to the machine/converter asymmetry, the unbalanced currents will also contain a negative sequence component,  $\vec{I}_{\alpha\beta-}$ . To illustrate a general case, the  $\alpha 1$ - $\beta 1$  and  $\alpha 2$ - $\beta 2$  currents are expressed as a sum of both positive and negative sequence components (it is assumed that there is no phase angle lead/lag between the components, for simplicity):

$$\begin{aligned}\vec{I}_{\alpha\beta 1} &= k_1 \vec{I}_{\alpha\beta+} + k_2 \vec{I}_{\alpha\beta-} = k_1 |\vec{I}_{\alpha\beta}| e^{+j\omega_s t} + k_2 |\vec{I}_{\alpha\beta}| e^{-j\omega_s t} \\ \vec{I}_{\alpha\beta 2} &= k_3 \vec{I}_{\alpha\beta+} + k_4 \vec{I}_{\alpha\beta-} = k_3 |\vec{I}_{\alpha\beta}| e^{+j\omega_s t} + k_4 |\vec{I}_{\alpha\beta}| e^{-j\omega_s t}\end{aligned}\quad (8)$$

Here  $\beta$ -axis leads  $\alpha$ -axis by  $90^\circ$  and anti-clockwise rotation is considered as the positive direction. Coefficients  $k_i$ ,  $i = 1, 2, 3, 4$ , depend on the type of the asymmetry.

Using the concept of the  $x$ - $y$  currents of Section II, the general expression for  $x$ - $y$  currents due to the machine/converter asymmetry can be deduced as:

$$\begin{aligned}\vec{I}_{xy} &= (k_1 - k_3) \vec{I}_{\alpha\beta} e^{-j\omega_s t} + (k_2 - k_4) \vec{I}_{\alpha\beta} e^{+j\omega_s t} \\ &= \vec{I}_{xy-} + \vec{I}_{xy+}\end{aligned}\quad (9)$$

It should be noted that the rotational direction has changed, due to the opposite polarity in  $x$ - and  $y$ -current equations (7); hence the positive sequence component in  $\alpha$ - $\beta$  plane appears as negative sequence component in  $x$ - $y$  plane, and vice versa.

It can be concluded from (9) that the  $x$ - $y$  currents, caused by machine/converter asymmetry, are of the fundamental frequency. Depending on the type of asymmetry, these  $x$ - $y$  currents can rotate in the synchronous, anti-synchronous or in both directions.

Three scenarios can be considered to illustrate the effect of machine/converter asymmetry on the  $x$ - $y$  currents:

**Case (A):** Three-phase currents in both windings are balanced, but with different magnitudes. Hence  $k_1 \neq k_3$ ;  $k_2 = k_4 = 0$ .

**Case (B):** Currents in winding 2 are balanced, but currents in winding 1 are unbalanced. Thus  $k_1 \neq k_3$ ;  $k_2 \neq 0$ ;  $k_4 = 0$ .

**Case (C):** Currents in both windings 1 and 2 have the same imbalance, so that  $k_1 = k_3$ ;  $k_2 \neq k_4$ .

The corresponding  $x$ - $y$  currents for the three scenarios are:

**Case (A):** only  $\vec{I}_{xy-}$  is present.

**Case (B):** both  $\vec{I}_{xy+}$  and  $\vec{I}_{xy-}$  are present.

**Case (C):** only  $\vec{I}_{xy+}$  is present.

By applying a pair of PI controllers to regulate the  $x$ - $y$  currents in the synchronous reference frame, the positive sequence component will appear as a dc quantity and hence it can be easily compensated. Similarly, control of the negative sequence component will be made possible if the PI controllers are implemented in an anti-synchronous reference frame. Hence, it is expected that Case (A) and (C) require PI control in the anti-synchronous reference frame and the synchronous reference frame, respectively, whereas Case (B) will require both synchronous and anti-synchronous PI controllers for the asymmetry compensation. This is in agreement with the analysis presented in [11].

Using the reverse analogy, by injecting the correct  $x$ - $y$  currents, the type of asymmetry can be induced as desired. In [12], the use was made of this concept by deliberately injecting anti-synchronous  $x$ - $y$  currents to create the necessary asymmetry for dc-link voltage balancing.

The investigation in [11] was restricted to simulations only. Here, experimental results are used instead to validate the discussion. The experimental study is done using four types of PI controllers which operate in different reference frames, namely, the stationary, synchronous, anti-synchronous and dual (synchronous and anti-synchronous) reference frame, as shown in Fig. 2.

### B. Dead-Time Compensation

The existence of inverter dead time introduces harmonics that distort the voltage and current. In the past, various methods have been proposed, especially for single and three-phase systems, where dead-time compensation has been made possible by the means of calculating and compensating the voltage error [13–15], or by the use of current control methods [10], [16]. The implementation of the former usually requires

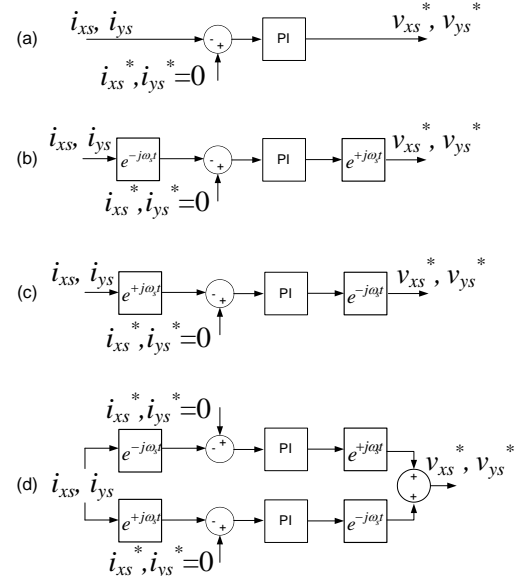


Fig. 2. PI current control of  $x$ - $y$  currents, implemented in different reference frames: (a) stationary reference frame (b) synchronous reference frame (c) anti-synchronous reference frame, and (d) dual (synchronous and anti-synchronous) reference frame.

knowledge of the system parameters and the phase current polarity, which causes difficulties in implementation. An interesting modification of the method was presented in [17] where the output from the  $d$ -axis PI controller was used to estimate the voltage error that needs to be compensated. However, the implementation requires multiple integrators with specific control. The current control approach, on the other hand, relies on current controller(s) to suppress the dead-time related harmonic currents and hence achieve dead-time compensation. This approach, which does not require specific calculation of the dead-time voltage error, is considered here.

The dominant dead-time harmonics in multiphase machines appear as ac components in the  $x$ - $y$  plane rather than in the  $d$ - $q$  plane. The effect of dead time can thus be more severe because the machine's impedance in the  $x$ - $y$  plane is low. It was shown in [10] that dead time caused harmonics in a five-phase induction machine can be suppressed by using synchronous PI current controllers in the  $x$ - $y$  plane. However, the PI controllers are unable to fully compensate ac components. Nonetheless, suppression of these components is made possible in [10] by using a high proportional gain  $K_p$  for the synchronous  $x$ - $y$  PI current controllers. The limitation of this approach is therefore the maximum value of  $K_p$ , which depends on factors such as computational and modulation delays.

Even though the dead time voltage can exhibit non-linear characteristics at low current level [18], a simple representation of the dead time effect as a square wave [13] is used in the discussion here. Using Fourier expansion, the square wave can be resolved into a series of odd order harmonics. For multiphase machines with multiple three-phase windings and mutually isolated neutrals, the third harmonic current cannot flow. Hence, the dominant dead time harmonics are the 5<sup>th</sup> and 7<sup>th</sup>.

An alternative to PI controllers is the use of resonant controllers. For a three-phase system, the 5<sup>th</sup> and the 7<sup>th</sup> harmonic currents appear as current vectors rotating with frequencies of  $-5\omega_s$  and  $+7\omega_s$  in the stationary reference frame, where  $\omega_s$  is the fundamental frequency. If a reference frame

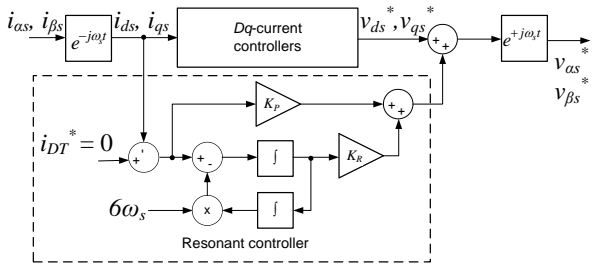


Fig. 3. Dead time compensator for a three-phase machine using resonant controller in the synchronous ( $d$ - $q$ ) reference frame.

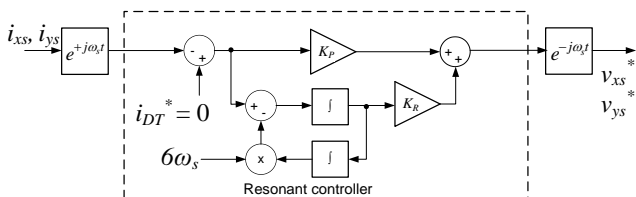


Fig. 4. Dead time compensator for an asymmetrical six-phase machine using resonant controller in the anti-synchronous ( $x$ - $y$ ) reference frame.

rotating with frequency  $+\omega_s$  is used, as is the case when vector control is implemented, these harmonics will appear as the  $-6^{\text{th}}$  and  $+6^{\text{th}}$  harmonics, respectively. These harmonics can hence be compensated using a single resonant controller tuned at  $6\omega_s$ . The concept of utilising such synchronous reference frame resonant (SRF-Res) controller for harmonic compensation has been successfully applied for applications involving three-phase active filters [19–22] and grid-tied converter [16], [23], where multiple SRF-Res controllers are used in parallel to compensate a wide range of harmonics. In [24], single SRF-Res controller is used to control a doubly-fed induction generator under distorted grid voltage. Here, this approach is adopted for dead time compensation in the drive. For a three-phase machine, the resonant controller can be added in parallel to the  $d$ - $q$  current controllers in the synchronous reference frame, as shown in Fig. 3.

The same dead time compensator can be applied for the asymmetrical six-phase machine. However, in this case the 5<sup>th</sup> and the 7<sup>th</sup> harmonics appear in the  $x$ - $y$  plane rather than in the  $d$ - $q$  plane, and rotate with frequencies  $+5\omega_s$  and  $-7\omega_s$ . In order to compensate for these dead time harmonics, it is therefore necessary to use resonant controller in the anti-synchronous reference frame instead. The structure of the dead time compensator for the six-phase machine using the resonant controller is shown in Fig. 4.

The use of resonant controllers has gained in popularity in recent times [25–30]. Since the resonant frequency is variable in this case, the two-integrator method is used to implement the resonant controller in the vector proportional-integral (VPI) form [26]. A comprehensive discussion of the improvement of frequency accuracy and stability margin of digital resonant controllers, by performing pole correction and delay compensation, is also available in [26]. Here, pole correction is provided by using the forth-order approximation (not shown in Fig. 4). Since the order of harmonics to be compensated is low, VPI resonant controller allows stable operation even without delay compensation.

Using this structure of the resonant controller, the gains  $K_p$  and  $K_R$  are selected on the basis of  $K_p/K_R = L_{Ls,xy}/R_{xy}$  of the  $x$ - $y$  plane.  $K_p$  is then selected to achieve desired selectivity and transient response of the controller [22]. A large  $K_p$  improves transient response but reduces selectivity, so a compromise between the two is necessary. Since the resonant dead time compensator is expected to operate in parallel with the other ( $x$ - $y$  current) controllers, the value of  $K_p$  is selected as sufficiently small to minimise the effect on the other controllers.

## IV. EXPERIMENTAL RESULTS AND DISCUSSION

### A. Experimental Setup Overview

Experimental tests are conducted on an asymmetrical six phase squirrel cage induction machine, configured with two isolated neutral points. It was obtained by rewinding a 1.1 kW, 380 V, 50 Hz machine, with rated current and speed of 1.75 A and 930 rpm, respectively. The machine is supplied using a custom-made eight-phase two-level voltage source converter (VSC), configured for six-phase operation. A dc power supply (Sorensen SGI 600-25) is used to provide the dc-link voltage of 300 V to the VSC. A 5 kW dc machine is mechanically

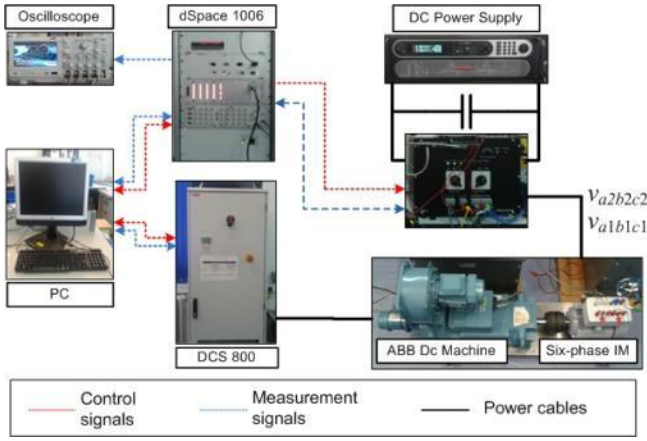


Fig. 5. Experimental setup for the asymmetrical six-phase induction motor drive testing.

TABLE I. EXPERIMENTAL SYSTEM PARAMETERS

Machine parameters			
$R_s = 12.5 \Omega$	$R_r = 12.0 \Omega$	$J = 0.04 \text{ kg}\cdot\text{m}^2$	$p = 3$
$L_{ls\_dq} = 0.0615 \text{ H}$	$L_{lr} = 0.0110 \text{ H}$	$L_m = 0.590 \text{ H}$	
$L_{ls\_xy} = 0.0055 \text{ H}$			
Converter Parameters			
$C_1 = C_2 = 1500 \mu\text{F}$	$V_{dc1} = V_{dc2} = 300 \text{ V}$		
Controller Parameters			
$f_{switching} = 5 \text{ kHz}$	$f_{sampling} = 10 \text{ kHz}$		
<b>D-q current controllers:</b>	$K_p = 60$	$K_i = 8000$	
<b>Speed controller:</b>	$K_p = 0.05$	$K_i = 0.05$	

coupled to the six-phase machine and is controlled using ABB DCS800 drive in the torque control mode, to provide loading onto the six-phase machine. The experimental setup is shown in Fig. 5.

The six-phase machine is controlled using indirect rotor flux oriented control (IRFOC) in closed-loop speed control mode. The double zero-sequence injection carrier-based PWM [8] is utilized. The complete control algorithm is implemented using dSpace DS1006 system. Switching frequency is 5 kHz, with 6  $\mu\text{s}$  dead time provided by the hardware in the VSC. Machine phase currents and dc-link voltage are measured (using the LEM sensors embedded in the VSCs) through dSpace at a sampling frequency of 10 kHz. Currents are filtered for display purposes using a low-pass filter with the cut-off frequency of 2 kHz. For variables such as  $x$ - $y$  currents and machine speed, the values are calculated within dSpace and displayed on the oscilloscope via DS2101 DAC module. To provide current display at higher resolution, current probe (TCP0030) and Tektronix oscilloscope (MSO2014) are used. The machine and control parameters are given in Table I.

The experimental results are presented in the following order: subsection B shows the effect of dead time compensation using PI controllers and the resonant controller. This helps to establish the effectiveness of the dead time compensation technique. Subsection C then discusses the asymmetry compensation capabilities of the PI controllers in different reference frames. In order to remove the dead time

harmonics from the currents, the dead time compensator of subsection B is used throughout the experiments in subsection C.

### B. Dead Time Compensator

In order to verify the performance of the resonant dead time compensator discussed in Section III, the controller is compared with the dead time compensation scheme of [10], based on PI controllers in the synchronous reference frame. Based on the considerations presented in Section III the resonant controller gains are selected as  $K_p = 1$  and  $K_R = 2272$ . For PI controllers, since the dead time compensation effect depends primarily on the proportional part of the controller, the proportional gain is tuned to be as high as possible without having the controller going into instability. Via trial and error,  $K_p$  is found to be 70 in this case. The integral gain, which has little effect on dead time harmonics, is chosen to be 2500.

The machine is at first operated at a constant speed of +500 rpm without load. The performance of different controllers is compared in Fig. 6. Fig. 6(a) shows the operation of the machine when only  $d$ - $q$  current controllers are used. Since no  $x$ - $y$  currents control is provided, the dead time harmonics are left uncompensated. FFT spectrum of the phase current (obtained by processing the oscilloscope data in Matlab) shows that the phase current contains harmonics with the dominant 5<sup>th</sup> and 7<sup>th</sup> order components. Fig. 6(b) shows the case when synchronous reference frame PI controllers of [10] are used. Results show significant improvement of the current waveform since harmonics in the  $x$ - $y$  currents have been reduced. FFT analysis shows that the 5<sup>th</sup> and the 7<sup>th</sup> harmonic currents have been suppressed to a good extent. The test is repeated next using stationary reference frame PI controllers with the same PI gains ( $K_p = 70$  and  $K_i = 2500$ ) and the results are shown in Fig 6(c). It is observed that the harmonic suppression capability is almost identical to the synchronous reference frame PI controllers. This shows that here the reference frame has little impact in terms of the dead time compensation (the dominant dead time harmonic in [10] is the 3<sup>rd</sup>, while here the dominant harmonics are at higher frequencies, the 5<sup>th</sup> and the 7<sup>th</sup>). The performance of the dead time compensator using the resonant controller is shown in Fig. 6(d). Compared with stationary and synchronous PI control, the resonant controller is able to provide much more effective compensation of the 5<sup>th</sup> and the 7<sup>th</sup> harmonics, which are in essence eliminated. The performance is good despite the small value of the gains used. This shows the superiority of the resonant dead time compensator over those based on PI controllers. It is worth noting that an improvement of total harmonic distortion (THD) is also observed with the dead time compensation (THD values are given in the headings of current spectra). Nevertheless, the improvement is small because the THD is dominated by the high order switching related harmonics, which largely depend on the choice of the pulse width modulation method [31].

The same set of tests is repeated for the machine operating at +250 rpm, and the results are shown in Fig. 7. Again, synchronous (Fig. 7(b)) and stationary (Fig. 7(c)) PI controllers show similar but limited harmonic suppression

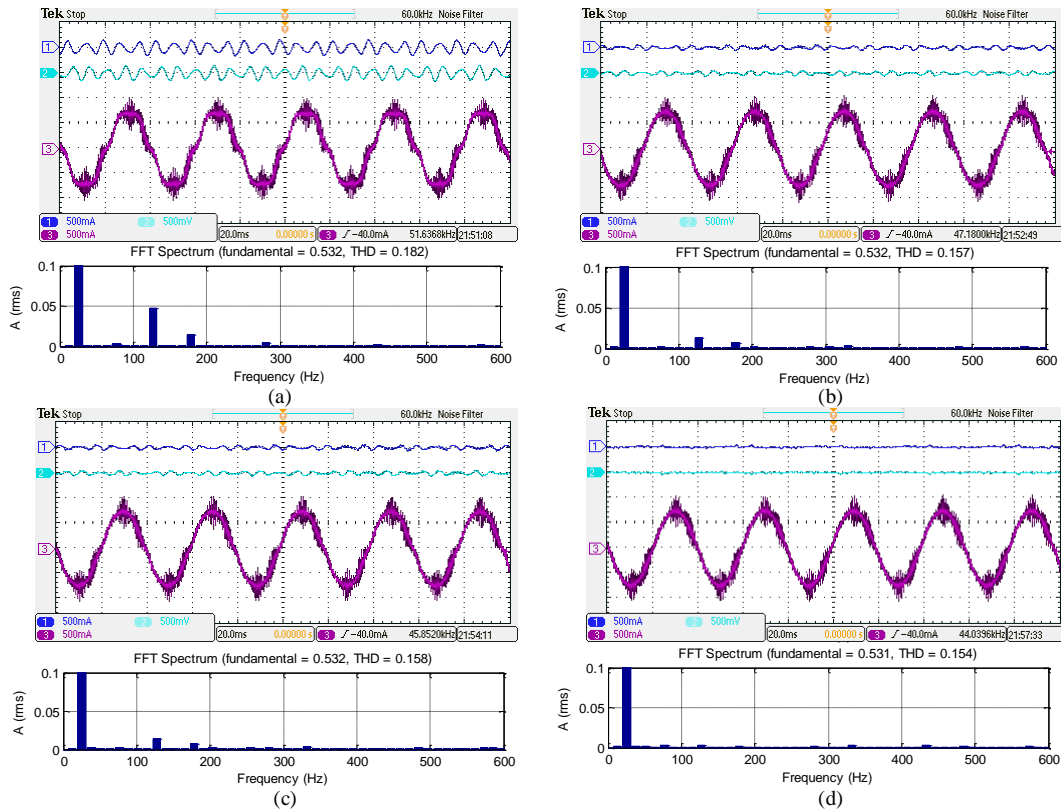


Fig. 6. Experimental results (with FFT spectrum of phase- $a1$  current) for no-load operation at 500 rpm with  $d-q$  current controllers and (a) no  $x-y$  current controllers (b)  $x-y$  current control using synchronous PI controllers (c)  $x-y$  current control using stationary PI controllers (d)  $x-y$  current control using synchronous resonant controller: Channel 1:  $i_x$  (0.5A/div), Channel 2:  $i_y$  (0.5A/div), Channel 3: phase- $a1$  current (0.5A/div), Horizontal: Time (20ms/div).

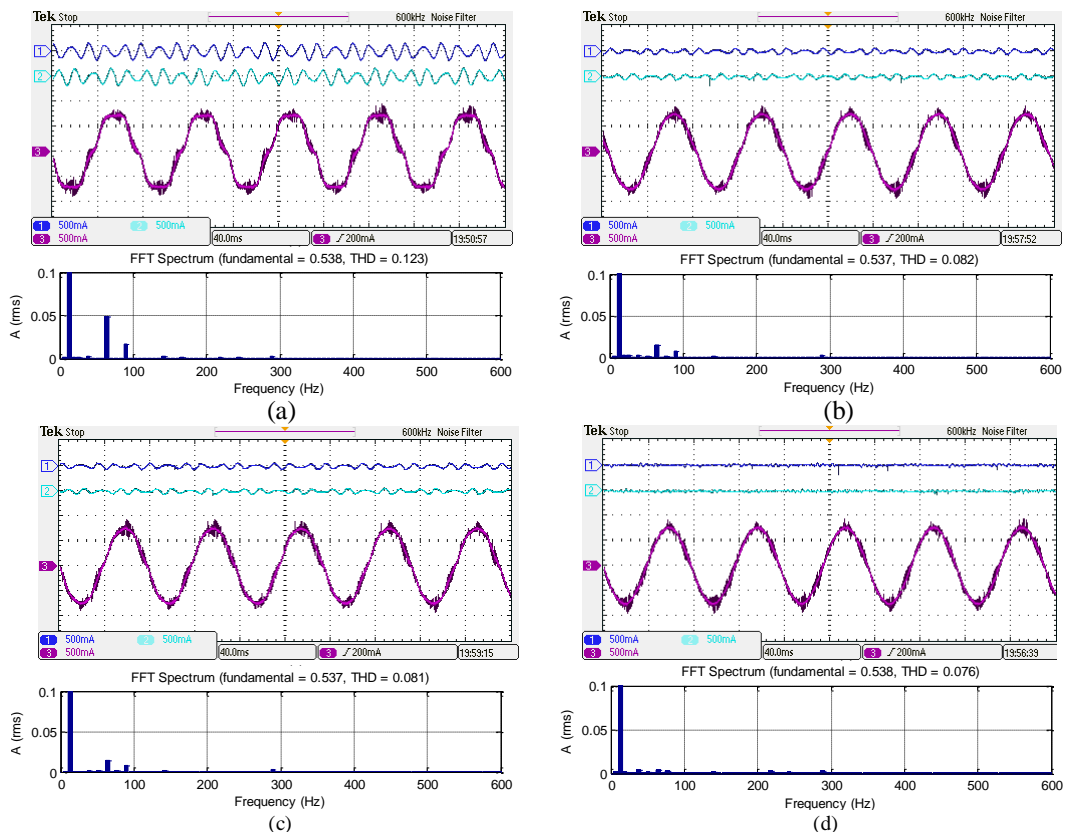


Fig. 7. Experimental results (with FFT spectrum of phase- $a1$  current) for no-load operation at 250 rpm with  $d-q$  current controllers and (a) no  $x-y$  current controllers (b)  $x-y$  current control using synchronous PI controllers (c)  $x-y$  current control using stationary PI controllers (d)  $x-y$  current control using synchronous resonant controller: Channel 1:  $i_x$  (0.5A/div), Channel 2:  $i_y$  (0.5A/div), Channel 3: phase- $a1$  current (0.5A/div), Horizontal: Time(40ms/div)

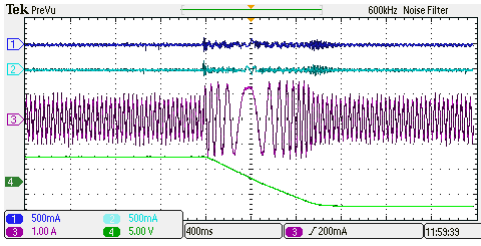


Fig. 8. Experimental results showing speed reversal (+500 rpm to -500 rpm) of the machine in no-load operation with resonant dead time compensator activated: Channel 1:  $i_x$  (0.5A/div), Channel 2:  $i_y$  (0.5A/div), Channel 3: phase- $a1$  current (1.0A/div), Channel 4: speed (500rpm/div), Horizontal: Time (400ms/div).

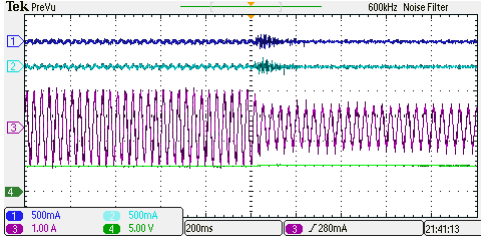


Fig. 9. Experimental results showing machine operating at +500 rpm with load torque removed at  $t = 1.0$  s: Channel 1:  $i_x$  (0.5A/div), Channel 2:  $i_y$  (0.5A/div), Channel 3: phase- $a1$  current (1.0A/div), Channel 4: speed (500rpm/div), Horizontal: Time (200ms/div).

capability, while the resonant controller (Fig. 7(d)) exhibits a far superior performance.

The dynamic performance of the dead time compensator is tested by reversing the speed of the machine from +500 rpm to -500 rpm. As shown in Fig. 8, the addition of the dead time compensator does not affect the speed control ( $d$ - $q$  current control) of the machine, and the system remains stable. It should be emphasised that the resonant controller only suppresses the 5<sup>th</sup> and the 7<sup>th</sup> order dead time harmonics, so a small amount of fundamental frequency component due to the inherent machine/converter asymmetry appears in the steady state  $x$ - $y$  currents.

Fig. 9 shows the performance of the dead time compensator when the machine's load torque is varied. The six-phase machine is at first loaded with 50% of the rated torque using the dc motor coupled to the machine. At  $t = 1.0$  s, the load torque is removed. Small oscillations in  $x$ - $y$  currents can be observed during transient due to the controller's limited response speed. Nevertheless, the controller is able to suppress the harmonics during steady state. Some small oscillations are again present in steady state as a result of the inherent machine/converter asymmetry.

### C. Asymmetry Compensation

This section shows the results of the machine/converter asymmetry compensation using PI controller in different reference frames for  $x$ - $y$  current control. As discussed above, depending on the type of the asymmetry, fundamental frequency  $x$ - $y$  currents will appear in the synchronous, anti-synchronous or both reference frames. It is expected that the synchronous PI controllers can eliminate the synchronous component, and the anti-synchronous PI controller will be able to compensate the anti-synchronous component. By observing the performance of the PI controllers, the type of components present in the  $x$ - $y$  currents can be concluded upon. Four types of PI controllers, all shown in Fig. 2 (stationary, synchronous,

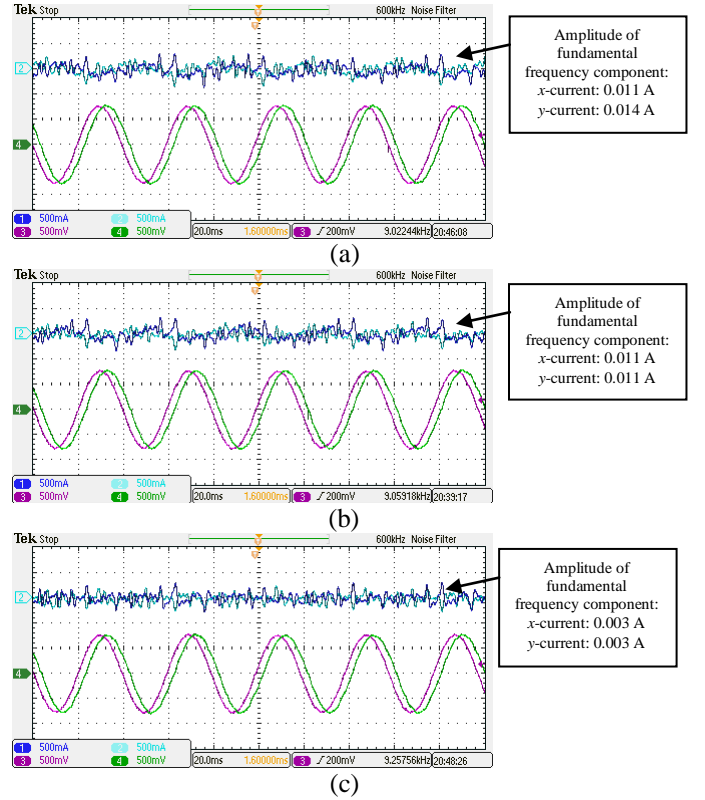


Fig. 10. Experimental results showing the inherent machine asymmetry, when machine runs at +500 rpm without load, with (a) no  $x$ - $y$  current control, and with  $x$ - $y$  current control using (b) synchronous PI (c) anti-synchronous PI control: Channel 1:  $i_x$  (0.05A/div), Channel 2:  $i_y$  (0.05A/div), Channel 3: phase- $a1$  current (0.5A/div), Channel 4: phase- $a2$  current (0.5A/div), Horizontal: Time (20ms/div). (Markers for Channel 1 and Channel 3 have been overlapped by markers from Channel 2 and Channel 4, respectively).

anti-synchronous and dual-synchronous reference frame PI controllers), are discussed in this section.

In order to suppress the harmonics due to the dead time effect, the resonant dead time compensator is activated in parallel with the PI controllers. PI controllers' gains are tuned in the following manner: the ratio of  $K_p/K_i$  is chosen to be equal to  $L_{ls\_xy}/R_{xy}$  to cancel out the dominant pole of the  $x$ - $y$  plane. In order to show a clearer effect of the reference frame and reduce the interference with the dead time compensator, a small value of  $K_p$  is chosen, i.e.  $K_p = 1$ . Cross-coupling effect is reduced by adding terms  $-\omega_s L_{ls\_xy} i_{ys}$  and  $+\omega_s L_{ls\_xy} i_{xs}$  to the outputs of the  $x$ - and  $y$ -controllers, respectively, using measured currents. It should be noted that, when dual PI controllers are used, these terms are unable to provide cross-coupling decoupling, since terms from synchronous and anti-synchronous controllers cancel each other. More sophisticated decoupling approaches, such as for example the use of complex PI [22], can overcome this problem; this is however beyond the scope of this paper.

In order to show the effect of asymmetry on phase currents in different windings, the currents of phase- $a1$  and phase- $a2$  are shown further on. The inherent asymmetry in the machine/converter is investigated first. The machine runs without load with the set speed of +500 rpm using IRFOC. Fig. 10(a) shows the  $x$ - $y$ , phase- $a1$  and phase- $a2$  currents when  $x$ - $y$  current control is not implemented (except for the dead time compensator, which eliminates dead time related 5<sup>th</sup> and 7<sup>th</sup>

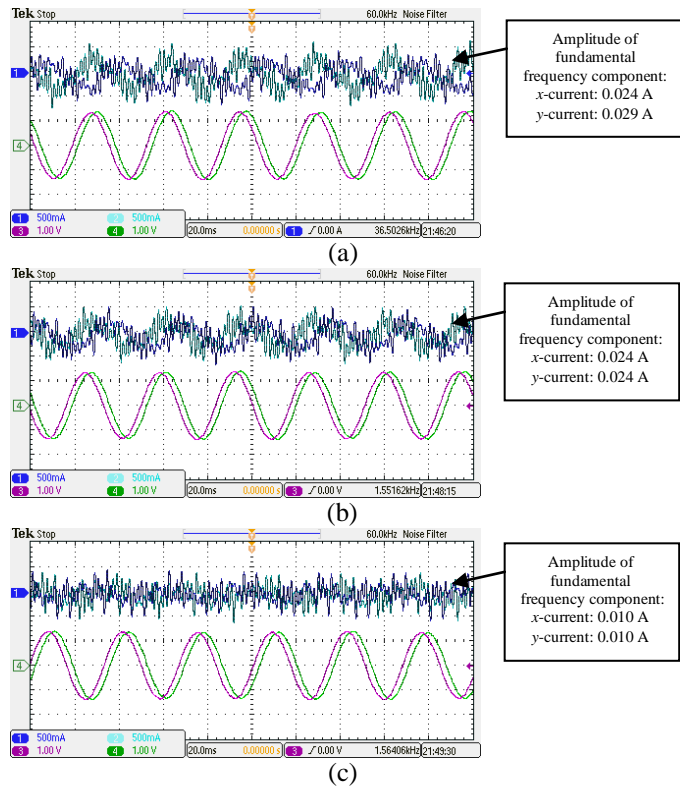


Fig. 11. Experimental results showing the inherent machine asymmetry, when machine runs at +500 rpm with 50% rated load, with (a) no  $x$ - $y$  current control, and with  $x$ - $y$  current control using (b) synchronous PI (c) anti-synchronous PI control: Channel 1:  $i_x$  (0.05A/div), Channel 2:  $i_y$  (0.05A/div), Channel 3: phase- $a1$  current (1.0A/div), Channel 4: phase- $a2$  current (1.0A/div), Horizontal: Time (20ms/div). (Markers for Channel 1 and Channel 3 have been overlapped by markers from Channel 2 and Channel 4, respectively).

harmonics). The ripples in the  $x$ - $y$  currents are mainly due to the machine/converter asymmetry and noise. From the figure, the inherent asymmetry is small in no-load operation. Fig. 10(b) and 10(c) show the results when synchronous PI and anti-synchronous PI  $x$ - $y$  current controllers are used. By comparing the fundamental frequency component in  $x$ - $y$  currents, it is found that anti-synchronous PI provides better compensation than the synchronous PI controller (which provides hardly any improvement). This indicates that the inherent asymmetries in this machine mainly produce anti-synchronous  $x$ - $y$  currents.

Fig. 11 shows the effect of machine loading by applying 50% of the rated torque to the machine, while keeping the speed at +500 rpm. Compared to Fig. 10, the amplitude of  $x$ - $y$  currents has increased because of the increase in the phase currents. The impact of adding the synchronous and anti-synchronous PI controllers can be observed in Fig. 11(b) and 11(c), respectively. Similar to the no-load case, anti-synchronous PI controllers provide better performance, confirming that the inherent asymmetry caused  $x$ - $y$  currents is predominantly of anti-synchronous type.

In order to verify the discussion in Section III, three types of asymmetry are emulated next, by adding external resistors in series with the stator windings. For Case (A), stator resistance in phases  $a1$ ,  $b1$  and  $c1$  is increased by  $5.7 \Omega$ . For Case (B), only the resistance in phase- $a1$  is increased by  $5.7 \Omega$ . For Case (C), resistors of  $5.7 \Omega$  are added in phase- $a1$  and phase- $a2$ . Since the inherent asymmetry is much smaller than the

emulated asymmetry, its effect can be considered now as negligible.

The experimental results are shown in Fig. 12. To facilitate the comparison, results for different types of asymmetry are placed in three separate columns, as indicated with the legend on the top of Fig. 12. Each row shows the results for one particular PI current control method in the  $x$ - $y$  plane. The speed is kept at +500 rpm. For simplicity, the machine is operated without load. The first row shows the results when only  $d$ - $q$  currents are controlled and no  $x$ - $y$  current control is provided. This is done by setting the  $x$ - $y$  voltage references to zero. This scenario would have been perfectly sufficient for the control of the drive had the inverter and the machine been ideal, as explained in [10] in conjunction with a five-phase machine. It can be observed that the different types of asymmetry introduce  $x$ - $y$  currents that are different not only in their magnitudes, but also in the phase relation between  $x$ - $y$  currents. By observing the lead-lag relation between the  $x$ - $y$  currents, the presence of synchronous and/or anti-synchronous component can be deduced. For Case (A),  $y$ -current leads  $x$ -current, indicating that the  $x$ - $y$  currents are mainly rotating in the anti-synchronous direction. The opposite can be observed for Case (C), where  $x$ -current is leading  $y$ -current. For Case (B), there is no obvious lead or lag relation between the  $x$ - and  $y$ -current, which implies that synchronous and anti-synchronous components of comparable magnitude are present. These observations show that the emulated asymmetries closely resemble those described in Section III.

Row (b) shows the results when stationary PI controllers are used to suppress the  $x$ - $y$  currents. Since all the  $x$ - $y$  currents appear as ac quantities in the stationary reference frame, there is practically no improvement over the case without  $x$ - $y$  current control. This is partly due to the fact that the controllers have been tuned with low bandwidth. Increasing controllers' gain would undoubtedly improve the performance, but full compensation of the  $x$ - $y$  currents cannot be achieved.

Row (c) shows the performance of synchronous PI controllers. For Case (A), the synchronous PI controllers are unable to compensate the anti-synchronous  $x$ - $y$  currents, since they appear as ac quantities with frequency of  $2\omega_s$  to the synchronous PI controllers. For Case (B), the synchronous PI controllers are capable of suppressing the synchronous  $x$ - $y$  current components. However, the uncompensated anti-synchronous component still flows in the machine, so the phase currents remain unbalanced. In Case (C), the  $x$ - $y$  currents appear as dc component to the synchronous PI controller and hence can be fully compensated.

The effect of anti-synchronous PI control is seen in row (d) of Fig. 12. It can be observed that the anti-synchronous PI controller is capable of eliminating the  $x$ - $y$  currents in Case (A) but not in Case (C) due to the fact that  $x$ - $y$  currents only contain anti-synchronous component in Case (A), and only synchronous component in Case (C). For Case (B), the anti-synchronous PI controllers only provide partial suppression of the asymmetrical currents, and the synchronous  $x$ - $y$  current components remain unsuppressed.

Row (e) shows the performance of the dual PI controllers. Since both synchronous and anti-synchronous PI controllers are present,  $x$ - $y$  currents can be effectively compensated in all the three cases. This shows that the dual PI controllers are

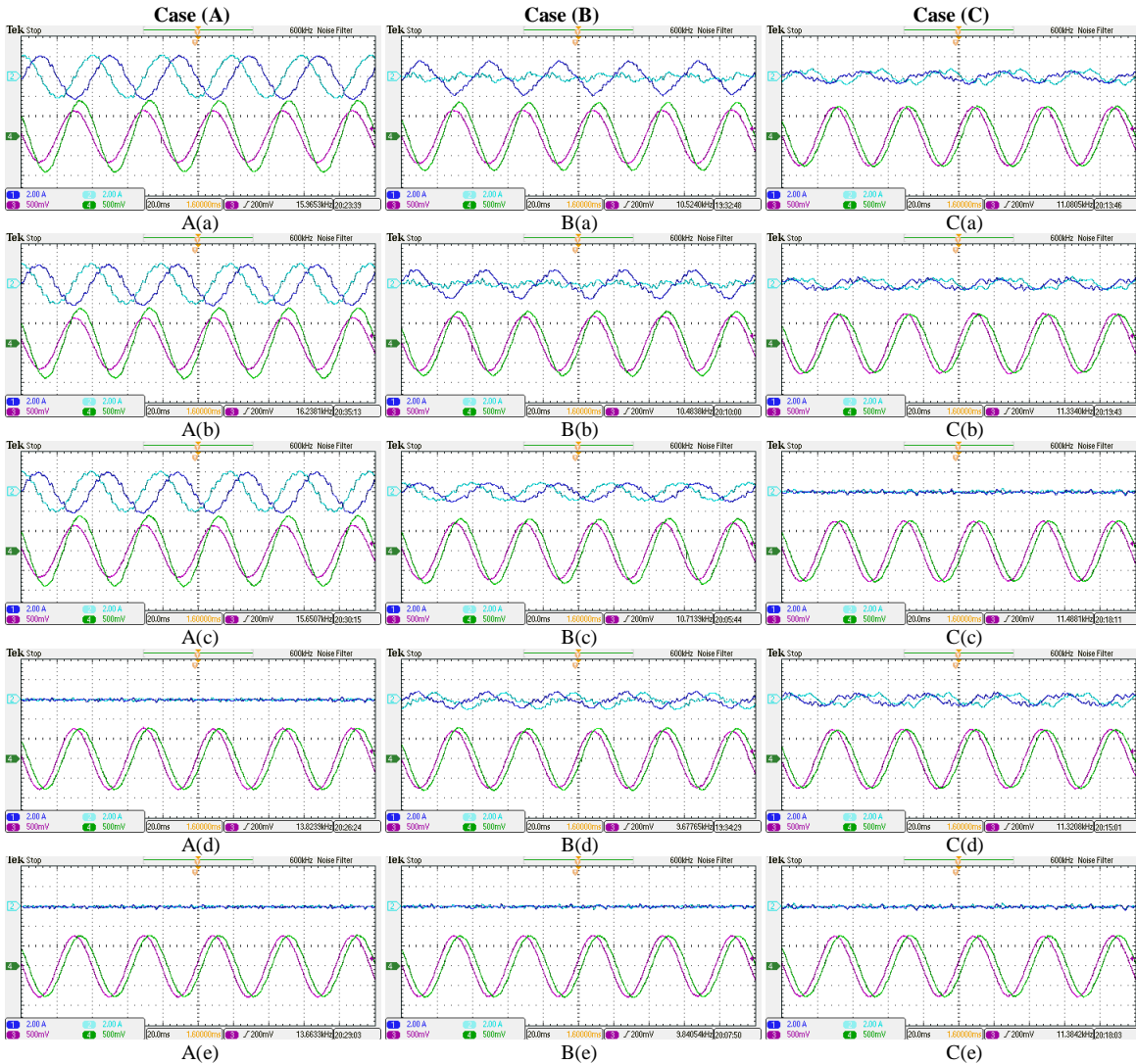


Fig. 12. Experimental results showing asymmetry compensation effect (a) without  $x$ - $y$  current control ( $x$ - $y$  voltage references set to zero), and with  $x$ - $y$  current control using (b) stationary PI (c) synchronous PI (d) anti-synchronous PI, and (e) dual PI controllers for Cases (A), (B) and (C): Channel 1:  $i_x$  (0.2A/div), Channel 2:  $i_y$  (0.2A/div), Channel 3: phase- $a1$  current (0.5A/div), Channel 4: phase- $a2$  current (0.5A/div), Horizontal: Time (20ms/div). (Markers for Channel 1 and Channel 3 have been overlapped by markers of Channel 2 and Channel 4, respectively).

naturally capable of eliminating any  $x$ - $y$  currents caused by the machine/converter asymmetry. Dual PI controllers are actually equivalent to a resonant controller in the stationary reference frame, with resonant frequency equal to the fundamental frequency.

On the basis of the presented results, it can be concluded that the  $x$ - $y$  current control based on a dual PI or resonant controllers is the best choice in terms of the machine/converter asymmetry compensation. The use of dual PI controller can also be useful to allow fault-tolerant control of the machine, as shown in [32]. However, the results also show that if the type of asymmetry is known, it is possible to achieve the same performance with just a single PI controller per axis in the correct reference frame.

## V. CONCLUSION

The paper shows that the  $x$ - $y$  currents in an asymmetrical six-phase machine can be physically interpreted as circulating currents between the two three-phase windings of the machine. By using this concept, the relation between the type of asymmetry in the machine/converter and the currents in the

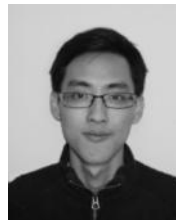
$x$ - $y$  plane has been established. Subsequently, two important aspects of the  $x$ - $y$  current control, i.e. asymmetries and dead-time compensation, have been discussed. For dead time compensation, a resonant controller implemented in the anti-synchronous reference frame shows the best performance, as proven on the basis of experimental results.

In terms of the asymmetry compensation, it is shown that the inherent machine/converter asymmetry produces  $x$ - $y$  currents that rotate at fundamental frequency. The  $x$ - $y$  currents can, however, rotate in the synchronous, anti-synchronous or both directions, depending on the type of the asymmetry present. The effectiveness of asymmetry compensation using PI controllers hence depends on the reference frame in which the control is implemented. Full compensation for all the possible cases is achievable only with the dual PI controllers (i.e. pairs in both synchronous and anti-synchronous reference frames). The validity of the discussion is verified by experimental results.

## REFERENCES

[1] E. Levi, R. Bojoi, F. Profumo, H. A. Toliyat, and S. Williamson,

- “Multiphase induction motor drives – a technology status review,” *IET Electric Power Applications*, vol. 1, no. 4, pp. 489–516, 2007.
- [2] E. Levi, “Multiphase electric machines for variable-speed applications,” *IEEE Trans. on Industrial Electronics*, vol. 55, no. 5, pp. 1893–1909, 2008.
- [3] T. A. Lipo, “A d-q model for six phase induction machines,” *Int. Conf. on Electrical Machines ICEM*, Athens, Greece, 1980, pp. 860–867.
- [4] G. K. Singh, K. Nam, and S. K. Lim, “A simple indirect field-oriented control scheme for multiphase induction machine,” *IEEE Trans. on Industrial Electronics*, vol. 52, no. 4, pp. 1177–1184, 2005.
- [5] Y. Zhao and T. A. Lipo, “Space vector PWM control of dual three-phase induction machine using vector space decomposition,” *IEEE Trans. on Industry Applications*, vol. 31, no. 5, pp. 1100–1109, 1995.
- [6] R. Bojoi, F. Profumo, and A. Tenconi, “Digital synchronous frame current regulation for dual three-phase induction motor drives,” *IEEE Conf. on Power Electronics Specialist PESC*, Acapulco, Mexico, 2003, vol. 3, pp. 1475–1480.
- [7] R. Bojoi, F. Farina, M. Lazzari, F. Profumo, and A. Tenconi, “Analysis of the asymmetrical operation of dual three-phase induction machines,” *IEEE Int. Electric Machines and Drives Conference IEMDC*, Madison, Wisconsin USA, 2003, pp. 429–435.
- [8] R. Bojoi, A. Tenconi, F. Profumo, G. Griva, and D. Martinello, “Complete analysis and comparative study of digital modulation techniques for dual three-phase AC motor drives,” *IEEE Power Electronics Specialists Conference PESC*, Cairns, Queensland, Australia, 2002, vol. 2, pp. 851–857.
- [9] R. Bojoi, E. Levi, F. Farina, A. Tenconi, and F. Profumo, “Dual three-phase induction motor drive with digital current control in the stationary reference frame,” *IEE Proceedings - Electric Power Application*, vol. 153, no. 1, pp. 129–139, 2006.
- [10] M. Jones, S. N. Vukosavic, D. Dujic, and E. Levi, “A synchronous current control scheme for multiphase induction motor drives,” *IEEE Trans. on Energy Conversion*, vol. 24, no. 4, pp. 860–868, Dec. 2009.
- [11] H. S. Che, W. P. Hew, N. A. Rahim, E. Levi, M. Jones, and M. J. Duran, “Current control of a six-phase induction generator for wind energy plants,” *15th International Power Electronics and Motion Control Conference, EPE-PEMC ECCE Europe*, 2012.
- [12] H. S. Che, W. P. Hew, N. A. Rahim, E. Levi, M. Jones, and M. J. Duran, “A Six-Phase Wind Energy Induction Generator System with Series-connected DC-links,” *IEEE Power Electronics for Distributed Generation Systems*, Aalborg, Denmark, 2012, pp. 26–33.
- [13] S. Jeong and M. Park, “The analysis and compensation of dead-time effects in PWM inverters,” *IEEE Trans. on Industrial Electronics*, vol. 38, no. 2, pp. 108–114, 1991.
- [14] Y. Wang, Q. Gao, and X. Cai, “Mixed PWM for dead-time elimination and compensation in a grid-tied inverter,” *IEEE Trans. on Industrial Electronics*, vol. 58, no. 10, pp. 4797–4803, 2011.
- [15] M. A. Herran, J. R. Fischer, A. Gonzalez, M. G. Judewicz, and D. O. Carrica, “Adaptive dead-time compensation for grid-connected PWM inverters of single-stage PV systems,” *IEEE Trans. on Power Electronics*, vol. 28, no. 6, pp. 2816–2825, 2013.
- [16] S.-H. Han, T.-H. Jo, J.-H. Park, H.-G. Kim, T.-W. Chun, and E.-C. Nho, “Dead time compensation for grid-connected PWM inverter,” *8th Int. Conf. on Power Electronics - ECCE Asia*, Jeju, South Korea, 2011, pp. 876–881.
- [17] S. Hwang and J. Kim, “Dead time compensation method for voltage-fed PWM inverter,” *IEEE Trans. on Energy Conversion*, vol. 25, no. 1, pp. 1–10, 2010.
- [18] J. M. Guerrero, M. Leetmaa, F. Briz, A. Zamarrón, and R. D. Lorenz, “Inverter nonlinearity effects in high-frequency signal-injection-based sensorless control methods,” *IEEE Trans. on Industry Applications*, vol. 41, no. 2, pp. 618–626, 2005.
- [19] R. I. Bojoi, G. Griva, V. Bostan, M. Guerriero, F. Farina, and F. Profumo, “Current control strategy for power conditioners using sinusoidal signal integrators in synchronous reference frame,” *IEEE Trans. on Power Electronics*, vol. 20, no. 6, pp. 1402–1412, 2005.
- [20] L. R. Limongi, R. Bojoi, G. Griva, and A. Tenconi, “Digital current-control schemes,” *IEEE Industrial Electronics Magazine*, vol. 3, no. 1, pp. 20–31, 2009.
- [21] R. Bojoi, L. R. Limongi, F. Profumo, D. Roiu, and A. Tenconi, “Analysis of current controllers for active power filters using selective harmonic compensation schemes,” *IEEJ Trans. on Electrical and Electronic Engineering*, vol. 4, no. 2, pp. 139–157, Mar. 2009.
- [22] C. Lascu, L. Asiminoaei, I. Boldea, and F. Blaabjerg, “High performance current controller for selective harmonic compensation in active power filters,” *IEEE Trans. on Power Electronics*, vol. 22, no. 5, pp. 1826–1835, Sep. 2007.
- [23] M. Liserre, R. Teodorescu, and F. Blaabjerg, “Multiple harmonics control for three-phase grid converter systems with the use of PI-RES current controller in a rotating frame,” *IEEE Trans. on Power Electronics*, vol. 21, no. 3, pp. 836–841, May. 2006.
- [24] C. Liu, F. Blaabjerg, W. Chen, and D. Xu, “Stator current harmonic control with resonant controller for doubly fed induction generator,” *IEEE Trans. on Power Electronics*, vol. 27, no. 7, pp. 3207–3220, 2012.
- [25] A. G. Yepes, F. D. Freijedo, J. Doval-Gandoy, O. Lopez, J. Malvar, and P. Fernandez-Comesana, “Effects of discretization methods on the performance of resonant controllers,” *IEEE Trans. on Power Electronics*, vol. 25, no. 7, pp. 1692–1712, 2010.
- [26] A. G. Yepes, F. D. Freijedo, O. Lopez, and J. Doval-Gandoy, “High-performance digital resonant controllers implemented with two integrators,” *IEEE Trans. on Power Electronics*, vol. 26, no. 2, pp. 563–576, 2011.
- [27] A. G. Yepes, F. D. Freijedo, O. Lopez, and J. Doval-Gandoy, “Analysis and design of resonant current controllers for voltage-source converters by means of Nyquist diagrams and sensitivity function,” *IEEE Trans. on Industrial Electronics*, vol. 58, no. 11, pp. 5231–5250, 2011.
- [28] S. A. Khajehoddin, M. Karimi-Ghartemani, P. K. Jain, and A. Bakshai, “A resonant controller with high structural robustness for fixed-point digital implementations,” *IEEE Trans. on Power Electronics*, vol. 27, no. 7, pp. 3352–3362, 2012.
- [29] B. P. McGrath and D. G. Holmes, “A General Analytical Method for Calculating Inverter DC-Link Current Harmonics,” *IEEE Trans. on Industry Applications*, vol. 45, no. 5, pp. 1851–1859, 2009.
- [30] R. Cardenas, C. Juri, R. Pena, P. Wheeler, and J. Clare, “The application of resonant controllers to four-leg matrix converters feeding unbalanced or nonlinear loads,” *IEEE Trans. on Power Electronics*, vol. 27, no. 3, pp. 1120–1129, 2012.
- [31] D. Dujic, M. Jones, and E. Levi, “Analysis of output current ripple RMS in multi-phase drives using polygon approach,” *IEEE Trans. on Power Electronics*, vol. 25, no. 7, pp. 1838–1849, 2010.
- [32] A. Tani, M. Mengoni, L. Zari, G. Serra, and D. Casadei, “Control of multiphase induction motors with an odd number of phases under open-circuit phase faults,” *IEEE Trans. on Power Electronics*, vol. 27, no. 2, pp. 565–577, 2012.



**Hang Seng Che** received his BEng degree in Electrical Engineering from the University of Malaya, Kuala Lumpur, Malaysia, in 2009. He is a recipient of the Kuok Foundation Postgraduate Scholarship Award for his PhD study, and is currently working towards his PhD degree under auspices of a dual PhD programme between the University of Malaya and Liverpool John Moores University. His research interests include multiphase machines and renewable energy.



**Emil Levi** (S'89, M'92, SM'99, F'09) received his M.Sc. and PhD degrees from the University of Belgrade, Yugoslavia in 1986 and 1990, respectively. From 1982 till 1992 he was with the Dept. of Elec. Engineering, University of Novi Sad. He joined Liverpool John Moores University, UK in May 1992 and is since September 2000 Professor of Electric Machines and Drives. He serves as Co-Editor-in-Chief of the *IEEE Trans. on Industrial Electronics*, as an Editor of the *IEEE Trans. on Energy Conversion*, and as Editor-in-Chief of the *IET Electric Power Applications*. Emil is the recipient of the Cyril Veinott award of the IEEE Power and Energy Society for 2009.



**Martin Jones** received his BEng degree (First Class Honours) in Electrical Engineering from the Liverpool John Moores University, UK in 2001. He was a research student at the Liverpool John Moores University from September 2001 till Spring 2005, when he received his PhD degree. Dr Jones was a recipient of the IEE Robinson Research Scholarship for his PhD studies and is currently with Liverpool John Moores University as a Reader. His research is in the area of high performance ac drives.



**Wooi-Ping Hew** obtained his BEng and Masters (Electrical) degrees from the University of Technology, Malaysia. He received his PhD from the University of Malaya, Kuala Lumpur, Malaysia in 2000. He is currently a Professor in the Faculty of Engineering, University of Malaya, Kuala Lumpur, Malaysia. Dr. Hew is a Member of IET and a Chartered Engineer. His research interests include electrical drives and electrical machine design.



**Nasrudin A. Rahim** (M'89–SM'08) received the B.Sc. (Hons.) and M.Sc. degrees from the University of Strathclyde, Glasgow, U.K., and the PhD degree from Heriot–Watt University, Edinburgh, U.K., in 1995. He is currently a Professor with the Faculty of Engineering, University of Malaya, Kuala Lumpur, Malaysia, where he is also the Director of the Power Energy Dedicated Advanced Center (UMPEDAC). Prof. Rahim is a Fellow of the IET, U.K., and the Academy of Sciences Malaysia.